*Article*

# The Effects of Cutting Parameters on Cutting Force and Tribological Properties of Machined Surface Under Dry Turning of AISI304L Austenitic Stainless Steel

**Gábor Kónya *** , **Béla Csorba** , **Norbert Szabó** and **Zsolt F. Kovács**

Department of Innovative Vehicles and Materials, GAMF Faculty of Engineering and Computer Science, John von Neumann University, Izsáki St. 10., H-6000 Kecskemét, Hungary; csorba.bela@nje.hu (B.C.); szabo.norbert@nje.hu (N.S.); kovacs.zsolt@nje.hu (Z.F.K.)
* Correspondence: konya.gabor@nje.hu

**Abstract:** In this study, the effects of cutting speed and feed rate on the roughness parameters $R_a$, $R_z$, $R_{sk}$, $R_{ku}$, $R_{pk}$, $R_{vk}$, and $A_2$ were examined during machining with coated carbide tools in a dry environment. The authors introduced the $R_{vk}/R_{pk}$ ratio, a coefficient that facilitates a simpler evaluation of surface wear resistance. Specifically, if this ratio is greater than 1, the surface is more wear-resistant, while values less than 1 indicate a higher tendency for surface wear. The Taguchi OA method was used to analyze and identify the significance of technological parameters on output characteristics. Based on the results, it was established that feed rate has the greatest impact on all output characteristics. The highest cutting force was measured at a cutting speed of 60 m/min and a feed rate of 0.15 mm/rev, attributed to the fact that at lower cutting speeds, the base material does not soften while the cross-sectional area of the chip increases. To achieve the lowest $R_a$ and $R_z$ surface roughness, a cutting speed of 100 m/min and a feed rate of 0.05 mm/rev are recommended. If the goal is to enhance surface wear resistance and improve oil retention capability, machining with a cutting speed of 80–100 m/min and a feed rate of 0.15 mm/rev is advisable, as the coarser machining increases both the $R_{vk}/R_{pk}$ ratio and the oil-retaining pocket size, which together improve the wear resistance of the machined surface.

**Keywords:** turning; stainless steel; cutting force; $R_a$; $R_z$; $R_{sk}$-$R_{ku}$ tribological map; $R_{pk}$; $R_{vk}$; $R_{vk}/R_{pk}$ ratio; $A_2$; dry machining

## 1. Introduction

The range of applications for austenitic steels is extensive. Leveraging their corrosion resistance properties, they are widely used in the automotive industry [1], the food industry [2], medical and laboratory instruments [3], and in the production of components [4]. Additionally, these steels are found in numerous other industries, including the chemical, mechanical, and construction industries [5–7]. Certain steel grades are particularly well-suited for marine piping systems, structures exposed to seawater (bridges and drilling platforms), heat exchangers, pressure vessels, and tanks [8,9]. The extensive and large-scale use of materials has also prompted the machinability of austenitic stainless steel to become a well-established scientific field with a history spanning several decades [10–14].

Stainless steels are classified as difficult-to-machine materials due to their tendency of work hardening, poor thermal conductivity, and high elongation. These properties result in increased cutting forces, more challenging chip formation, intense tool wear, built-up edge, and poorer surface quality [15–18]. Consequently, a significant portion of research focuses on reducing cutting forces [19], tool wear [20], vibration [21], and energy consumption [22] to improve efficiency by optimizing cutting parameters [23], tool coatings and geometries [24,25], and cooling-lubrication methods [26]. However, when considering the studies, the surface quality of the workpiece often receives less emphasis, as it fundamentally affects

the component's applicability and performance. Therefore, it is essential to examine this because, whether in mass production or small-batch manufacturing, many companies find it increasingly difficult to ensure the desired dimensional accuracy and surface quality during production while also meeting increasingly stringent process safety requirements. Hence, the measurement, analysis, and evaluation of surface quality in machined surfaces remain an important research field to this day [27–30]. In practice, surface quality is typically defined using the two most basic roughness parameters: the average roughness ($R_a$) and mean roughness depth ($R_z$) [31]. Although these parameters provide insight into the nature of a surface, they do not reveal significant differences between surface profiles.

Technological innovations have created new opportunities for more efficient evaluation of engineering surfaces, which, due to their complexity, are often described using statistical methods. The roughness characteristics of the surface formed during machining fundamentally determine the tribological behavior of the affected surface [32–35]. Therefore, in addition to the previously mentioned parameters, numerous other parameters provide valuable information about the roughness profiles of surfaces machined by different processes. These include, for example, the mean spacing of irregularities ($R_{Sm}$) or the root mean square slope of the profile ($R_{dq}$). $R_{Sm}$ is a longitudinal parameter, while $R_{dq}$ is a hybrid parameter. Using phenomenological models, the $R_a$, $R_z$, and $R_t$ values can be estimated, and based on this estimation, a topographical map of the machined surfaces can be generated, where the statistical parameters of the machined surfaces can be defined. These parameters include skewness ($R_{sk}$) and kurtosis ($R_{ku}$). With these two parameters, topographical maps of surfaces machined by different technologies can be established, where the $R_{sk}$-$R_{ku}$ values strongly depend on the cutting technology used [36–38]. $R_{sk}$ and $R_{ku}$ roughness values are widely used in the automotive industry, for instance, to characterize the cylinder walls of internal combustion engines, where both good wear resistance and adequate lubrication are crucial [39]. Skewness ($R_{sk}$) provides a relative comparison of the machined surface, measuring the "fill" of the profile. It can be positive or negative. Skewness is positive when the peaks of the profile are higher than the depths of the valleys, in which case $R_{sk} > 0$. Such surfaces may include planed or milled surfaces. Skewness is negative ($R_{sk} < 0$) when the valleys are deeper than the peaks. This suggests that the machined surface has better wear resistance and load-bearing capacity, which can be seen, for example, in mirror-polished surfaces [40]. When $R_{sk} = 0$, the surface profile can be considered normally distributed. This parameter provides a very important practical characteristic of the functional surface. Another important statistical parameter is kurtosis ($R_{ku}$), which describes the sharpness of the height distribution and measures the "sharpness" of the profile. $R_{ku} = 3$ in the case of a normal distribution. When $R_{ku} > 3$, the surface is sharp, and intense wear is present between the two sliding surfaces [41]. When $R_{ku} < 3$, the surface is blunt, leading to more favorable functional characteristics [42]. The $R_{pk}$ peak height represents the thickness of the rapidly wearing layer, while the $R_{vk}$ reduced valley depth reflects the surface's capacity to retain lubricants and wear particles. The primary objective is maintaining a greater $R_{vk}$ value than $R_{pk}$ [43,44]. Evaluating the $A_2$ parameter is essential, as it influences oil retention and the re-lubrication of the affected surface. A larger $A_2$ pocket enables more oil to be retained per unit area, which is especially important for gears [45].

In the machining of stainless steels, few studies have investigated the impact of machining input parameters on the surface roughness characteristics of the machined surface. In numerous studies, predictive models for $R_a$ roughness have been developed, investigating the technological parameters of $R_a$ and $R_z$ roughness parameters [46–50]. Leppert examined the effects of cutting speed, feed rate, and depth of cut on the $R_a$, $R_{sk}$, $R_{ku}$, $R_{pk}$, and $R_{vk}$ roughness parameters during the turning of AISI 316L stainless steel with a coated carbide insert under dry, emulsion, and minimum quantity lubrication (MQL) conditions. The results indicated that feed rate had the most significant impact on the roughness parameters among the technological parameters. When comparing cooling and lubrication methods, it was found that MQL yielded the best results within

the examined range of technological parameters [51]. Liu and colleagues investigated the effects of technological parameters on vibration and $R_a$ roughness during the turning of 304L stainless steel with a PVD-coated carbide tool under emulsion and minimum quantity cooling lubrication (MQCL) conditions. Based on the results, it was found that at higher cutting speeds and with identical feed rates, there was no difference in the performance of the cooling media in terms of $R_a$ roughness and vibration. Feed rate was also identified as having the greatest impact on $R_a$ roughness; as feed rate increased, $R_a$ also increased [21].

After reviewing the literature, it can be concluded that the investigation of roughness characteristics formed by turning stainless steels is still far from comprehensive. Therefore, in this study, the authors examined the effects of cutting speed and feed rate on cutting force and on the $R_a$, $R_z$, $R_{sk}$, $R_{ku}$, $R_{vk}$, $R_{pk}$, and $A_2$ roughness parameters during the dry turning of 1.4306 austenitic stainless steel with a coated carbide insert. Additionally, they introduced the $R_{vk}/R_{pk}$ ratio as a simplified measure of a surface's wear resistance; if this ratio is greater than 1, the surface is more wear-resistant, and if less than 1, it is less wear-resistant. To determine the clear significance of the technological parameters, the Taguchi OA method was applied. This information is particularly useful for components used in the automotive industry.

## 2. Materials and Methods

The turning tests were carried out on an NCT BNC-446 type CNC lathe. For the machining process, a TaeguTec-manufactured CNMG 120408 EM TT9225 insert with a TiCN-Al$_2$O$_3$-TiCN CVD coating was used in a PCLNR 2020 K12 tool holder. A coated tool was chosen for the machining tests because coatings reduce the coefficient of friction between the tool and the workpiece material, thereby enabling a smoother surface finish during machining [52–55]. Coatings can significantly enhance the wear resistance of tools, which is also crucial for the surface integrity and tribological properties of the machined surface [56]. The determination of the range of technological parameters was based on supplier recommendations. The significance of technological parameters was determined using the Taguchi experimental design method. The Taguchi Orthogonal Array (OA) is particularly suitable for efficiently reducing the number of experiments defined by the factors and levels influencing the process, thereby decreasing the number of experiments and the time required [57]. The Taguchi method evaluates the quality of the machining output using the signal-to-noise (S/N) ratio, with its selection depending on the output parameter being investigated. In this study, the output parameters are cutting force, $R_a$, $R_z$, $R_{sk}$, $R_{ku}$, $R_{pk}$, $R_{vk}$, and $A_2$. The goal is primarily to minimize these values, except for the $R_{vk}$ and $A_2$ parameters, where higher values are preferred. Therefore, the "smaller is better" S/N ratio was calculated using Equation (1), while the "larger is better" S/N ratio was calculated using Equation (2) [58].

$$S/N = (-10) \times \log\left(\frac{\sum y^2}{n}\right) \tag{1}$$

$$S/N = (-10) \times log\left(\frac{\sum \frac{1}{y^2}}{n}\right) \tag{2}$$

where *Y* represents the responses for the given factor-level combination and *n* represents the number of responses in the factor-level combination [58].

For the experimental design, an L9 Orthogonal Array was used (Table 1), which does not reduce the number of experiments in this case but is highly useful for determining the significance of the factors. The experimental design is shown in Table 2. The depth of cut was 1.5 mm, the machining length was 25 mm, and the initial diameter of the workpieces was 50 mm. Each experiment was carried out under dry conditions.

**Table 1.** Taguchi L9 orthogonal array parameter design.

| Factors | Levels |
|---|---|
| Cutting speed, $v_c$ (m/min) | 60; 80; 100 |
| Feed rate, $f$ (mm/rev.) | 0.05; 0.1; 0.15 |

**Table 2.** Experimental design.

| Run No. | Cutting Speed, $v_c$ (m/min) | Feed Rate, $f$ (mm/rev.) |
|---|---|---|
| 1 | 60 | 0.05 |
| 2 | 60 | 0.1 |
| 3 | 60 | 0.15 |
| 4 | 80 | 0.05 |
| 5 | 80 | 0.1 |
| 6 | 80 | 0.15 |
| 7 | 100 | 0.05 |
| 8 | 100 | 0.1 |
| 9 | 100 | 0.15 |

The experiments were conducted on 1.4306 (X2CrNi19-11, AISI 304L)-grade stainless steel, with the chemical composition, mechanical, and physical properties of the material shown in Tables 3 and 4. The chemical composition was determined using a FOUNDRY-MASTER PRO type spectrometer.

**Table 3.** The chemical composition of 1.4306 (X2CrNi19-11, AISI 304L) [59].

| Fe | C | Si | Mn | Cr | Ni | Co | Cu |
|---|---|---|---|---|---|---|---|
| 71.2 | 0.03 | 0.12 | 1.38 | 17.9 | 8.00 | 0.11 | 0.48 |

**Table 4.** The mechanical and physical properties of 1.4306 (X2CrNi19-11, AISI 304L) [60].

| Tensile Strength, $R_m$ (MPa) | Elongation, $A_5$ (%) | Hardness *HB* | Thermal Conductivity, $\lambda$ (W/m·K) |
|---|---|---|---|
| 629 | 42 | 218 | 15 |

During machining, force measurements were performed using a KISTLER 9257B type 3-component piezoelectric dynamometer, with a KISTLER 5007-type charge-amplifier unit. The force signals were recorded as a function of machining time using Dynoware® software (3.2.5.0), and these were later evaluated in OriginPro 2021® software. The sampling frequency was set so that for each experimental setup, a force signal would be measured for every 3° rotation of the workpiece. The determination of this was based on Equation (3) [59], and the calculated and rounded sampling frequency for each cutting speed is shown in Table 5.

$$f = \frac{n \cdot 120}{60} \ (\text{Hz}) \tag{3}$$

**Table 5.** The calculated and rounded sampling frequency for each cutting speed.

| Cutting Speed, $v_c$ (m/min) | C. Sampling Frequency, (Hz) | R. Sampling Frequency, (Hz) |
|---|---|---|
| 60 | 813.118 | 814 |
| 80 | 1084.157 | 1085 |
| 100 | 1355.197 | 1356 |

The tribological characteristics of the machined surfaces were measured three times on each surface using a Mitutoyo Formtracer SV-C3100-type tactile roughness tester, with the workpiece being rotated by $120°$ between each measurement.

## 3. Results

This section presents the effects and significance of the technological parameters, namely the cutting speed and feed rate on the cutting force, as well as on the $R_a$, $R_z$, $R_{sk}$, $R_{ku}$, $R_{pk}$, $R_{vk}$, and $A_2$ tribological parameters, and chip breaking.

### 3.1. Cutting Force

The analysis of cutting force is a critical aspect of machining science as several conclusions can be drawn from its magnitude and trends. Cutting forces have an impact on energy consumption, tool wear, and the surface quality of the machined workpiece [61]. The effect of feed rate on the cutting force ($F_c$) for each cutting speed, as well as the significance of the technological parameters on the cutting force ($F_c$), is shown in Figure 1. It is observed that the feed rate has a dominant effect on the cutting force as the increased chip cross-section due to higher feed rates in this cutting speed range requires greater cutting force. The lowest cutting force was measured at a cutting speed of 60 m/min and a feed rate of 0.05 mm/rev., while the highest cutting force was recorded during turning at a cutting speed of 60 m/min and a feed rate of 0.15 mm/rev. In dry machining, the importance of selecting the correct cutting speed becomes more dominant at higher feed rates as the softening of the chip requires a higher cutting temperature with larger chip cross-sections. This temperature is primarily influenced by the cutting speed.
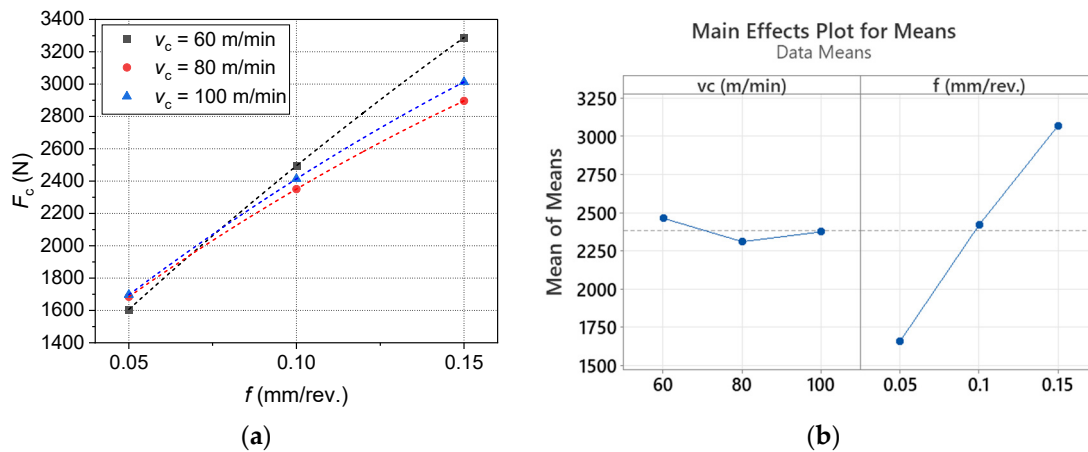


**Figure 1.** (**a**) The effect of feed rate in the case of each cutting speed on $F_c$ cutting force; (**b**) the significance of cutting parameters on $F_c$ cutting force.

### 3.2. Tribological Properties

#### 3.2.1. $R_a$, $R_z$

In most studies, $R_a$ and $R_z$ are commonly characterized, as these two roughness parameters are most often used in industry. However, there are application areas where knowledge of additional roughness parameters is essential as they determine specific functional characteristics. The general aim, both in the literature and in industry, is to minimize these roughness values. However, when other roughness parameters are considered, this statement may not always hold true. The effect and significance of the technological parameters on the $R_a$ and $R_z$ roughness parameters can be seen in Figures 2 and 3. The significance of the feed rate is clear, with cutting speed playing only a secondary role. It can be observed that as the feed rate increases, the $R_a$ increases, which is partly due to the tool marks on the machined surface. Additionally, for these materials, higher feed rates generate higher cutting forces and greater vibrations, both of which also affect surface roughness.

Minimal differences were observed between the actual measured results and the Taguchi analysis results. Based on the input factors and their levels, the Taguchi analysis suggests a cutting speed of 100 m/min and a feed rate of 0.05 mm/rev. However, a slightly better average surface roughness was measured at a cutting speed of 60 m/min, albeit within almost standard deviation. The difference in $R_z$ is somewhat larger than in $R_a$, which can be attributed to the fact that $R_z$ is more sensitive to vibrations than $R_a$. However, if the material removal rate (MRR) is considered, a cutting speed of 100 m/min and a feed rate of 0.05 mm/rev is more favorable.
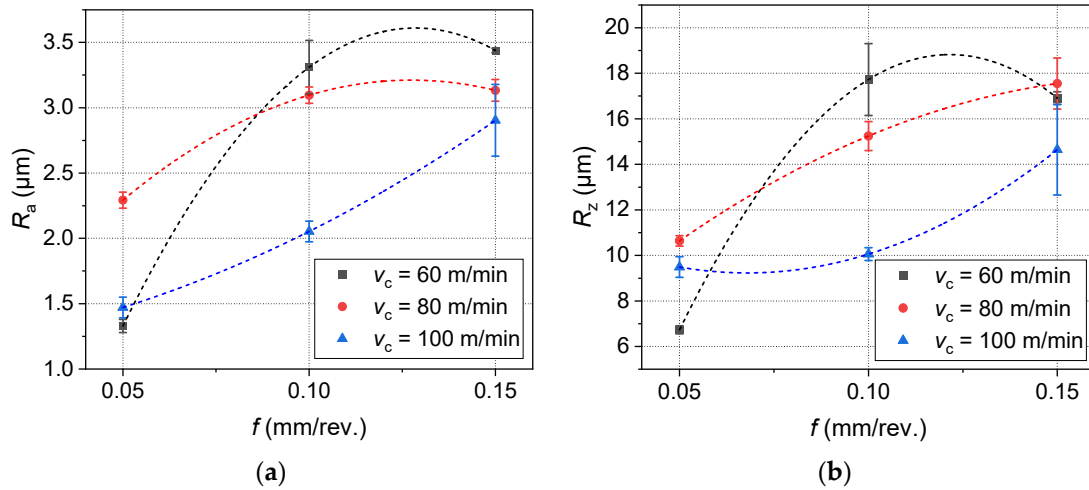


**Figure 2.** The effect of feed rate in the case of each cutting speed on (**a**) $R_a$ and (**b**) $R_z$ roughness parameters.
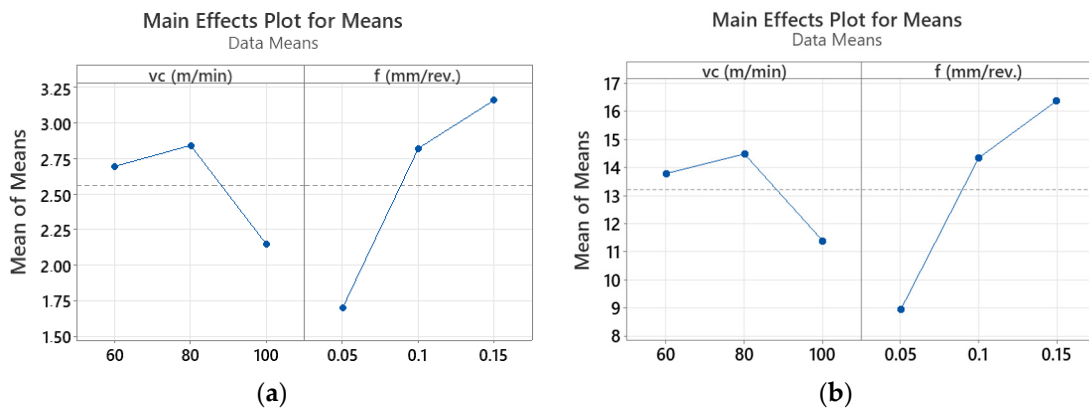


**Figure 3.** The significance of cutting parameters on (**a**) $R_a$ and (**b**) $R_z$ roughness parameters.

### 3.2.2. $R_{sk}$–$R_{ku}$

The $R_{sk}$–$R_{ku}$ tribological map is an excellent tool for positioning different technologies or various technological settings within one technology [34]. The $R_{sk}$–$R_{ku}$ tribological map is shown in Figure 4, while the significance of technological parameters on the $R_{sk}$ and $R_{ku}$ tribological parameters can be seen in Figure 5. For the $R_{sk}$ and $R_{ku}$ tribological parameters, smaller measured values are more favorable. It is widely accepted that the $R_{ku}$ should be less than 3, and according to this criterion, the surfaces machined with the 2., 6., and 7. technological parameter settings are not acceptable, as they exceed this value. For $R_{sk}$, the feed rate has a greater effect, while for $R_{ku}$, cutting speed is more influential. An optimum can be observed for both parameters at a cutting speed of 80 m/min, and in both cases, the feed rate produced more favorable results. Based on the tribological map, the best surface was achieved with the 4. experimental setting. The significance of the achieved results is further enhanced by the fact that, on a conventional tribological map [36], the lower $R_{sk}$ value for turning is typically around 0.2. In contrast, significant reductions were achieved

under various technological settings. The greatest improvement was observed with the 3. experimental setup, where the $R_{sk}$ value was reduced by approximately 0.5.
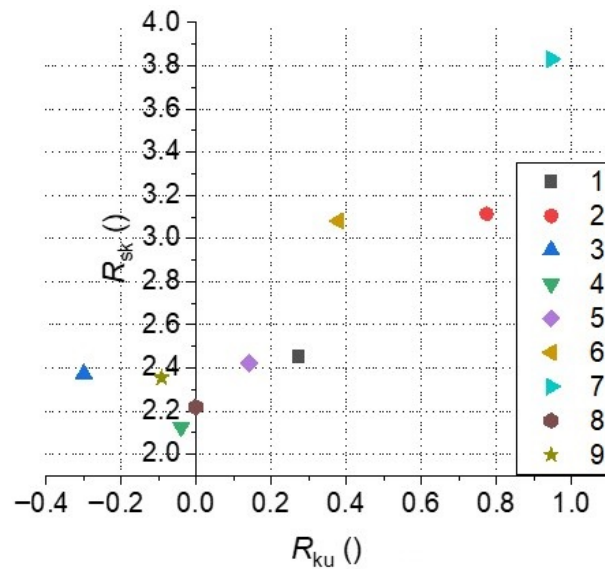


**Figure 4.** The $R_{sk}$–$R_{ku}$ tribological map.
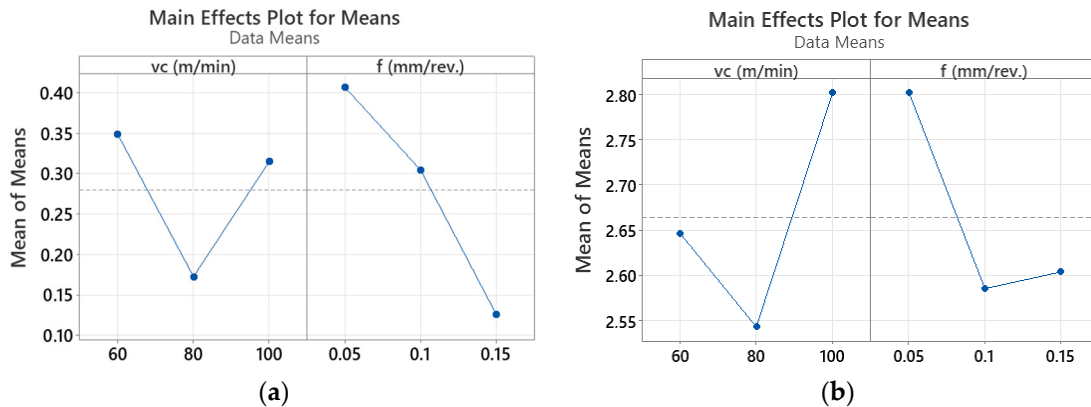


**Figure 5.** The significance of cutting parameters on (**a**) $R_{sk}$ and (**b**) $R_{ku}$ tribological parameters.

### 3.2.3. $R_{pk}$, $R_{vk}$, and $A_2$

The $R_{pk}$ and $R_{vk}$ roughness parameters are excellent for predicting the wear resistance of a surface, while $A_2$ is crucial for the oil retention capacity of the machined surface. In the evaluation of the Taguchi experimental design, the "smaller is better" formula was used for $R_{pk}$, as the goal is to minimize the peak heights, whereas for $R_{vk}$ and $A_2$, the "larger is better" formula was applied since the aim here is to find a combination of technological parameters that increases the values of these tribological characteristics. The comparison of $R_{pk}$, $R_{vk}$, and the $R_{vk}/R_{pk}$ ratio for different technological parameters, as well as the significance of these parameters for the characteristics, is shown in Figures 6–8. The primary goal is for the valleys to be deeper than the peaks, as this is the fundamental requirement for increasing the wear resistance of the part. This is achieved when the $R_{vk}/R_{pk}$ ratio is greater than 1. This requirement was met with the 3., 5., 6., 7., and 9. experimental setups. In the other settings, wear resistance decreases as a result. Figure 6 shows that increasing the technological parameters results in greater surface variability. Taking this factor into account, the 7. experimental setup is the most suitable if the goal is to improve these roughness values. Feed rate has the most significant effect on both parameters; however, for a smaller $R_{pk}$, a lower feed rate is recommended, while for a larger $R_{vk}$, a higher feed rate should be used. It is worth noting that a higher feed rate improves $R_{vk}$

more significantly than it worsens $R_{pk}$ in dry machining. Therefore, the higher cutting forces and vibrations that occur during machining help improve the difference between the two tribological characteristics.
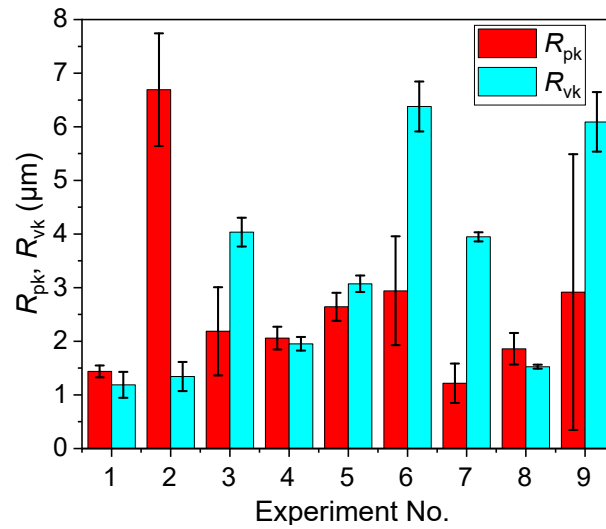


**Figure 6.** $R_{pk}$ and $R_{vk}$ as a function of cutting speed and feed rate.
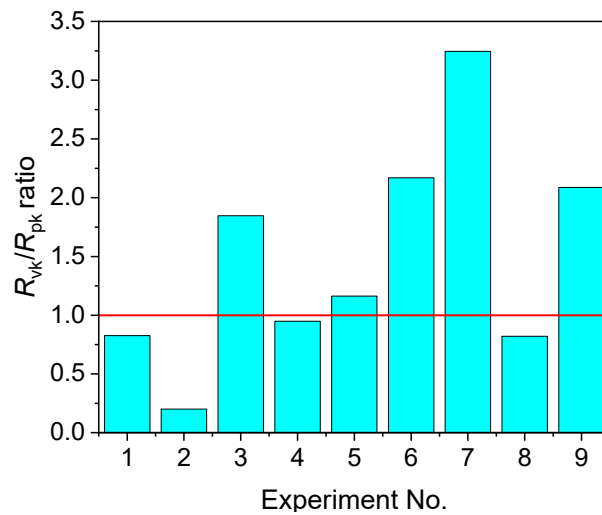


**Figure 7.** $R_{vk}/R_{pk}$ ratio as a function of cutting speed and feed rate.
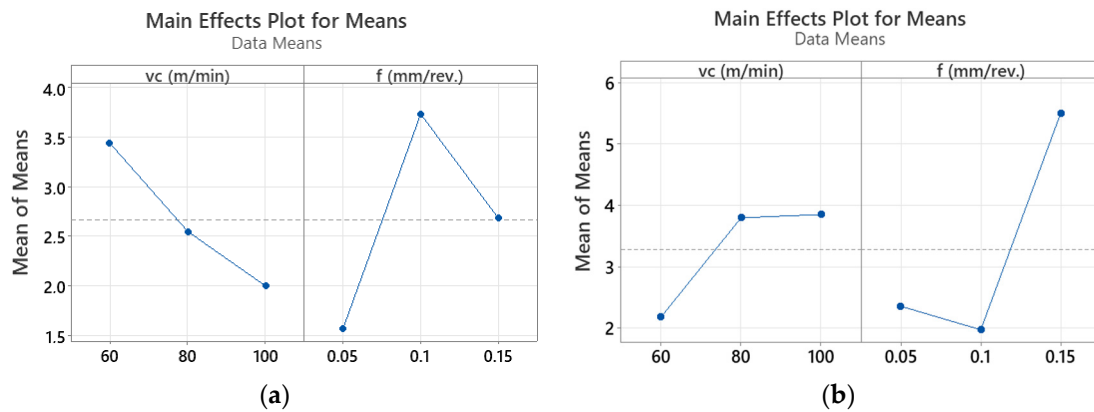


**Figure 8.** The significance of cutting parameters on (**a**) $R_{pk}$ and (**b**) $R_{vk}$.

The $A_2$ parameter is closely related to the other two parameters, and its dependence on the technological parameters, along with the significance of the technological parameters influencing it, is shown in Figure 9. The significance of the feed rate stands out as a higher feed rate results in a greater valley depth due to the tool marks, the increase in cutting force, and vibrations. The highest $A_2$ parameter was measured at a cutting speed of 60 m/min and a feed rate of 0.15 mm/rev. However, based on the Taguchi analysis, a cutting speed of 80 m/min is more favorable. This is because, at this cutting speed, the $A_2$ value remained almost constant as a function of the feed rate.



**(a)** **(b)**
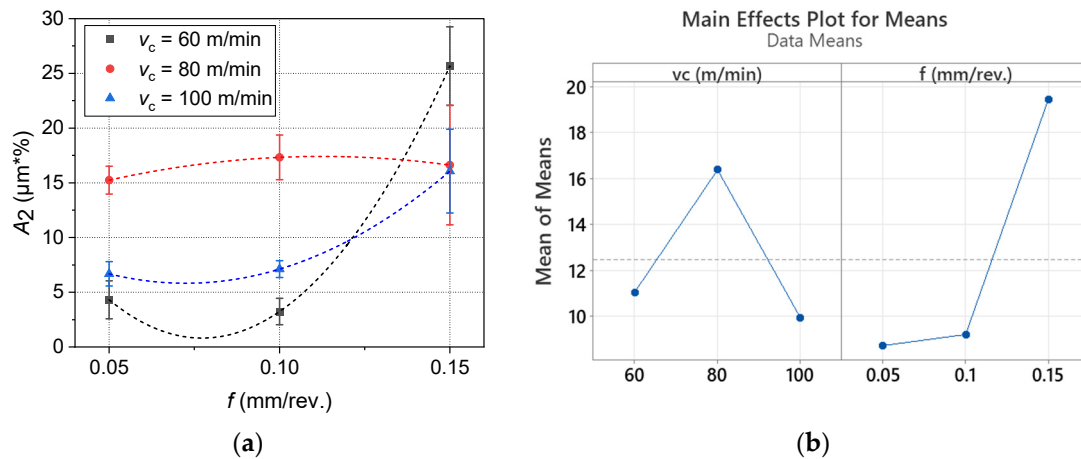
**Figure 9.** (**a**) The effect of feed rate in the case of each cutting speed on $A_2$ parameter; (**b**) the significance of cutting parameters on $A_2$.

## 4. Conclusions

In this paper, the authors investigated the effect of cutting speed and feed rate on cutting force, as well as on the surface roughness parameters $R_a$, $R_z$, $R_{sk}$, $R_{ku}$, $R_{pk}$, $R_{vk}$, and $A_2$, during dry turning of AISI304L austenitic stainless steel. In the field of stainless-steel machining, information on the examined roughness parameters has not yet been fully explored, thus providing sufficiently new insights for both science and industry. The authors graphically represented the $R_{vk}/R_{pk}$ ratio, which readily demonstrates the wear resistance of the machined surfaces. The authors stated the following conclusions:

- Within the examined parameter range, feed rate had the greatest influence on cutting force as the increased chip cross-section requires a higher forming force during chip removal. The lowest cutting force was measured during turning at a cutting speed of 60 m/min and a feed rate of 0.05 mm/rev.
- For the surface roughness parameters, it can be concluded that no single set of technological parameters can yield optimal values for all roughness parameters. The specific application of the part will determine which roughness parameters should be prioritized.
- For the $R_a$ and $R_z$ roughness parameters, the feed rate has the greatest influence—the smaller the feed rate, the lower the values of these parameters. If the focus is on these parameters, it is advisable to work with a low feed rate and higher cutting speed, as these parameters are highly sensitive to vibrations and cutting force, which have a negative impact on them. Considering the material removal rate (MRR) as well, a cutting speed of 100 m/min and a feed rate of 0.05 mm/rev. are recommended.
- The $R_{sk}$ tribological parameter is most affected by feed rate, while the $R_{ku}$ tribological parameter is primarily influenced by cutting speed. The most favorable conditions for both parameters are a cutting speed of 80 m/min and a higher feed rate. Compared to the 0.2 $R_{sk}$ minimum value represented on the conventional tribological map for turning, the $R_{sk}$ value was reduced by 0.5.

- For the $R_{pk}$, $R_{vk}$, and $A_2$ parameters, the feed rate also has a more significant impact. Considering all three parameters, the most favorable conditions are a cutting speed of 100 m/min and a feed rate of 0.15 mm/rev., which suggests that the higher cutting force and vibrations caused by the larger chip cross-section have a beneficial effect on these tribological parameters.

## References

1. Santacreu, P.; Glez, J.; Chinouilh, G.; Fröhlich, T. Behaviour Model of Austenitic Stainless Steels for Automotive Structural Parts. *Steel Res. Int.* **2006**, *77*, 686–691. [CrossRef]
2. Dewangan, A.K.; Patel, A.D.; Bhadania, A.G. Stainless steel for dairy and food industry: A review. *J. Mater. Sci. Eng.* **2015**, *4*, 5. [CrossRef]
3. Narayan, R.J. Medical Applications of Stainless Steels. In *Materials for Medical Devices*; Narayan, R.J., Ed.; ASM Handbook; ASM International: Almere, The Netherlands, 2015; Volume 3, pp. 199–210.
4. Dewidar, M.M.; Khalil, K.A.; Lim, J.K. Processing and mechanical properties of porous 316L stainless steel for biomedical applications. *Trans. Nonferrous Met. Soc. China* **2007**, *17*, 468–473. [CrossRef]
5. Gedge, G. Structural uses of stainless steel—Buildings and civil engineering. *J. Constr. Steel Res.* **2008**, *64*, 1194–1198. [CrossRef]
6. Gardner, L.; Nethercot, D.A. Structural stainless steel design: A new approach. *Struct. Eng.* **2004**, *82*, 21–28.
7. Yuan, J.; Ou, Z. Research Progress and Engineering Applications of Stainless Steel-Reinforced Concrete Structures. *Adv. Civ. Eng.* **2021**, *2021*, 9228493. [CrossRef]
8. Nagy, A.I.; Fábián, E.R.; Horváth, R.; Terek, P. Erősen ötvözött duplex korrózióálló acélok száraz forgácsolási nehézségei. *Műszaki Tudományos Közlemények* **2019**, *11*, 141–144. Available online: https://www.eme.ro/publication-hu/mtk/mtk11/MTK11-31-Nagy-Fabian-HorvathR-Terek.pdf (accessed on 30 October 2024).
9. Gamarra, J.R.; Diniz, A.E. Taper turning of super duplex stainless steel: Tool life, tool wear and workpiece surface roughness. *J. Braz. Soc. Mech. Sci. Eng.* **2018**, *40*, 39. [CrossRef]
10. Kosa, T.; Ney, R.P. *Machining of Stainless Steels*; ASM International: Almere, The Netherlands, 1989.
11. Fernández-Abia, A.I.; García, J.B.; López de Lacalle, L.N. 2-High-performance machining of austenitic stainless steels. In *Machining and Machine-Tools*; Davim, J.P., Ed.; Mechanical Engineering Series; Woodhead Publishing: Sawston, UK, 2013; pp. 29–90.
12. Kaladhar, M.; Subbaiah, K.V.; Rao, C.H.S. Machining of austenitic stainless steels—A review. *Int. J. Mach. Mach. Mater.* **2012**, *12*, 178. [CrossRef]
13. Fernández-Abia, A.I.; Barreiro, J.; López de Lacalle, L.N.; Martínez-Pellitero, S. Behavior of austenitic stainless steels at high speed turning using specific force coefficients. *Int. J. Adv. Manuf. Technol.* **2012**, *62*, 505–515. [CrossRef]
14. Gouveia, R.M.; Silva, F.J.G.; Reis, P.; Baptista, A.P.M. Machining Duplex Stainless Steel: Comparative Study Regarding End Mill Coated Tools. *Coatings* **2016**, *6*, 51. [CrossRef]
15. Monkova, K.; Monka, P.P.; Sekerakova, A.; Tkac, J.; Bednarik, M.; Kovac, J.; Jahnatek, A. Research on Chip Shear Angle and Built-Up Edge of Slow-Rate Machining EN C45 and EN 16MnCr5 Steels. *Metals* **2019**, *9*, 956. [CrossRef]
16. Maeng, S.; Ahn, J.H.; Min, B.-K. Effect of the Built-Up-Edge on Tool Wear in Machining of STAVAX. *Int. J. Precis. Eng. Manuf.* **2024**, *25*, 1375–1384. [CrossRef]
17. Yaman, K.; Tekiner, Z. Investigation of the effect of built-up edge on chip morphology at the cutting edge during turning operation. *Politek. Derg.* **2024**. Available online: https://dergipark.org.tr/en/download/article-file/3711315 (accessed on 30 October 2024).
18. Liu, D.; Ni, C.; Wang, Y.; Zhu, L. Review of serrated chip characteristics and formation mechanism from conventional to additively manufactured titanium alloys. *J. Alloys Compd.* **2024**, *970*, 172573. [CrossRef]
19. Osička, K.; Zouhar, J.; Sliwková, P.; Chladil, J. Cutting Force When Machining Hardened Steel and the Surface Roughness Achieved. *Appl. Sci.* **2022**, *12*, 22. [CrossRef]
20. Xavior, M.A.; Adithan, M. Determining the influence of cutting fluids on tool wear and surface roughness during turning of AISI 304 austenitic stainless steel. *J. Mater. Process. Technol.* **2009**, *209*, 900–909. [CrossRef]
21. Liu, N.; Liu, B.; Jiang, H.; Wu, S.; Yang, C.; Chen, Y. Study on vibration and surface roughness in MQCL turning of stainless steel. *J. Manuf. Process.* **2021**, *65*, 343–353. [CrossRef]
22. Korkmaz, M.E.; Günay, M. Finite Element Modelling of Cutting Forces and Power Consumption in Turning of AISI 420 Martensitic Stainless Steel. *Arab. J. Sci. Eng.* **2018**, *43*, 4863–4870. [CrossRef]

23. Su, Y.; Zhao, G.; Zhao, Y.; Meng, J.; Li, C. Multi-Objective Optimization of Cutting Parameters in Turning AISI 304 Austenitic Stainless Steel. *Metals* **2020**, *10*, 2. [CrossRef]
24. Rizzo, A.; Goel, S.; Luisa Grilli, M.; Iglesias, R.; Jaworska, L.; Lapkovskis, V.; Novak, P.; Postolnyi, B.O.; Valerini, D. The Critical Raw Materials in Cutting Tools for Machining Applications: A Review. *Materials* **2020**, *13*, 1377. [CrossRef] [PubMed]
25. Bobzin, K. High-performance coatings for cutting tools. *CIRP J. Manuf. Sci. Technol.* **2017**, *18*, 1–9. [CrossRef]
26. Haldar, B.; Joardar, H.; Louhichi, B.; Alsaleh, N.A.; Alfozan, A. A Comparative Machinability Study of SS 304 in Turning under Dry, New Micro-Jet, and Flood Cooling Lubrication Conditions. *Lubricants* **2022**, *10*, 359. [CrossRef]
27. Ercetin, A.; Aslantaş, K.; Özgün, Ö.; Perçin, M.; Chandrashekarappa, M.P.G. Optimization of Machining Parameters to Minimize Cutting Forces and Surface Roughness in Micro-Milling of Mg13Sn Alloy. *Micromachines* **2023**, *14*, 1590. [CrossRef]
28. Ganesh, V.D.; Bommi, R.M. Cutting force and surface roughness measurement in turning of Monel K 500 using GRA method. *Mater. Today Proc.* **2023**, *in press*.
29. Asiltürk, İ.; Kuntoğlu, M.; Binali, R.; Akkuş, H.; Salur, E. A Comprehensive Analysis of Surface Roughness, Vibration, and Acoustic Emissions Based on Machine Learning during Hard Turning of AISI 4140 Steel. *Metals* **2023**, *13*, 437. [CrossRef]
30. Yang, H.; Zheng, H.; Zhang, T. A review of artificial intelligent methods for machined surface roughness prediction. *Tribol. Int* **2024**, *199*, 109935. [CrossRef]
31. Kónya, G.; Kovács, Z.F. Effects of Oil Concentration in Flood Cooling on Cutting Force, Tool Wear and Surface Roughness in GTD-111 Nickel-Based Superalloy Slot Milling. *J. Manuf. Mater. Process.* **2024**, *8*, 119. [CrossRef]
32. Pawlus, P.; Reizer, R.; Żelasko, W. Two-Process Random Textures: Measurement, Characterization, Modeling and Tribological Impact: A Review. *Materials* **2022**, *15*, 268. [CrossRef]
33. Whitehouse, D.J. *Handbook of Surface and Nanometrology*; CRC Press: Boca Raton, FL, USA, 2011.
34. Kovács, Z.F.; Viharos Zs, J.; Kodácsy, J. Improvements of surface tribological properties by magnetic assisted ball burnishing. *Surf. Coat. Technol.* **2022**, *437*, 128317. [CrossRef]
35. Kovács, Z.F.; Viharos, Z.J.; Kodácsy, J. Surface flatness and roughness evolution after magnetic assisted ball burnishing of magnetizable and non-magnetizable materials. *Measurement* **2020**, *158*, 107750. [CrossRef]
36. Ruzzi, R.d.S.; da Silva, L.R.R.; da Silva, R.B.; da Silva Junior, W.M.; Bianchi, E.C. Topographical analysis of machined surfaces after grinding with different cooling-lubrication techniques. *Tribol. Int.* **2020**, *141*, 105962. [CrossRef]
37. Bhushan, B. *Modern Tribology Handbook*, 2nd ed.; Bhushan, B., Ed.; CRC Press LLC: Boca Raton, FL, USA, 2001; pp. 49–114.
38. Czifra, Á.; Bárányi, I. Sdq-Sdr Topological Map of Surface Topographies. *Front. Mech. Eng* **2020**, *6*, 50. [CrossRef]
39. da Silva, L.R.; Couto, D.A.; dos Santo, F.V.; Duarte, F.J.; Mazzaro, R.S.; Veloso, G.V. Evaluation of machined surface of the hardened AISI 4340 steel through roughness and residual stress parameters in turning and grinding. *Int. J. Adv. Manuf. Technol.* **2020**, *107*, 791–803. [CrossRef]
40. Grzesik, W.; Żak, K. Modification of surface finish produced by hard turning using superfinishing and burnishing operations. *J. Mater. Process. Technol.* **2012**, *212*, 315–322. [CrossRef]
41. Sedláček, M.; Podgornik, B.; Vižintin, J. Influence of surface preparation on roughness parameters, friction and wear. *Wear* **2009**, *266*, 482–487. [CrossRef]
42. Wongsue, S.; Thanatvarakorn, O.; Prasansuttiporn, T.; Nimmanpipug, P.; Sastraruji, T.; Hosaka, K.; Foxton, R.M.; Nakajima, M. Effect of surface topography and wettability on shear bond strength of Y-TZP ceramic. *Sci. Rep.* **2023**, *13*, 18249. [CrossRef]
43. Gadelmawla, E.S.; Koura, M.M.; Maksoud, T.M.A.; Elewa, I.M.; Soliman, H.H. Roughness parameters. *J. Mater. Process. Technol.* **2002**, *123*, 133–145. [CrossRef]
44. Dzierwa, A.; Markopoulos, A.P. Influence of Ball-Burnishing Process on Surface Topography Parameters and Tribological Properties of Hardened Steel. *Machines* **2019**, *7*, 11. [CrossRef]
45. Mikoleizig, G. Surface roughness measurements of cylindrical gears and bevel gears on gear inspection machines. *Gear Technol.* **2015**, *5*, 48–55.
46. Acayaba, G.M.A.; de Escalona, M. Prediction of surface roughness in low speed turning of AISI316 austenitic stainless steel. *CIRP J. Manuf. Sci. Technol.* **2015**, *11*, 62–67. [CrossRef]
47. Çaydaş, U.; Ekici, S. Support vector machines models for surface roughness prediction in CNC turning of AISI 304 austenitic stainless steel. *J. Intell. Manuf.* **2012**, *23*, 639–650. [CrossRef]
48. de Oliveira Junior, C.A.; Diniz, A.E.; Bertazzoli, R. Correlating tool wear, surface roughness and corrosion resistance in the turning process of super duplex stainless steel. *J. Braz. Soc. Mech. Sci. Eng* **2014**, *36*, 775–785. [CrossRef]
49. Bouzid, L.; Boutabba, S.; Yallese, M.A.; Belhadi, S.; Girardin, F. Simultaneous optimization of surface roughness and material removal rate for turning of X20Cr13 stainless steel. *Int. J. Adv. Manuf. Technol.* **2014**, *74*, 879–891. [CrossRef]
50. Selvaraj, D.P.; Chandramohan, P.; Mohanraj, M. Optimization of surface roughness, cutting force and tool wear of nitrogen alloyed duplex stainless steel in a dry turning process using Taguchi method. *Measurement* **2014**, *49*, 205–215. [CrossRef]
51. Leppert, T. Surface layer properties of AISI 316L steel when turning under dry and with minimum quantity lubrication conditions. *Proc. Inst. Mech. Eng. Part B J. Eng. Manuf.* **2012**, *226*, 617–631. [CrossRef]
52. Nobel, C.; Hofmann, U.; Klocke, F.; Veselovac, D.; Puls, H. Application of a new, severe-condition friction test method to understand the machining characteristics of Cu–Zn alloys using coated cutting tools. *Wear* **2015**, *344–345*, 58–68. [CrossRef]
53. Sahoo, P.; Patra, K. Cumulative reduction of friction and size effects in micro milling through proper selection of coating thickness of TiAlN coated tool: Experimental and analytical assessments. *J. Manuf. Process.* **2021**, *67*, 635–654. [CrossRef]

54. Özbek, N.A. Optimization of flank wear and surface quality in the turning of 1.2343 tool steel using carbide tools coated via different methods. *Surf. Topogr. Metrol. Prop.* **2021**, *9*, 025028. [CrossRef]

55. Keblouti, O.; Boulanouar, L.; Azizi, M.W.; Yallese, M.A. Effects of coating material and cutting parameters on the surface roughness and cutting forces in dry turning of AISI 52100 steel. *Struct. Eng. Mech.* **2017**, *61*, 519–526. [CrossRef]

56. Pang, X.; Zhang, B.; Li, S.; Zeng, Y.; Liu, X.; Shen, P.; Li, Z.; Deng, W. Machining performance evaluation and tool wear analysis of dry cutting austenitic stainless steel with variable-length restricted contact tools. *Wear* **2022**, *504–505*, 204423. [CrossRef]

57. Mia, M.; Dhar, N.R. Optimization of surface roughness and cutting temperature in high-pressure coolant-assisted hard turning using Taguchi method. *Int. J. Adv. Manuf. Technol.* **2017**, *88*, 739–753. [CrossRef]

58. Methods and Formulas for Analyze Taguchi Design. Available online: https://support.minitab.com/en-us/minitab/help-and-how-to/statistical-modeling/doe/how-to/taguchi/analyze-taguchi-design/methods-and-formulas/methods-and-formulas/ (accessed on 6 October 2024).

59. Kónya, G.; Takács, J.; Miskolcz, I.I.; Kovács, Z.F. Sciendo Investigation of the effects of machining parameters on cutting conditions during orthogonal turning of austenite stainless steel. *Prod. Eng. Arch.* **2024**, *30*, 86–93. [CrossRef]

60. Costa, C.E.; Polli, M.L. Effects of the infeed method on thread turning of AISI 304L stainless steel. *J. Braz. Soc. Mech. Sci. Eng.* **2021**, *43*, 253. [CrossRef]

61. Binali, R.; Demirpolat, H.; Kuntoğlu, M.; Salur, E. Different Aspects of Machinability in Turning of AISI 304 Stainless Steel: A Sustainable Approach with MQL Technology. *Metals* **2023**, *13*, 1088. [CrossRef]